Environment Protection Engineering

Vol. 52 2026 No. 1

DOI: 10.37190/epe/211197

HAO WANG[1], YU WANG (ORCID: 0000-0001-5621-6052)[1, 2, 3]
YING ZHANG[4], KAIQING LIU[4], TIAN-FENG LUO[5], TIAN MIAO[4]
MIAO TIAN[1], YUN WEI[4], XIAOLONG ZHANG[1], WEILONG REN[1]

AEOLIAN SAND TRANSPORT AND SEDIMENTATION PATTERNS IN NORTHWESTERN CHINA'S LOW-PRESSURE AREAS

Based on data collected from September to November in a single year, this study investigates the effects of wind speed, wind direction, topography, and seasonal variations on aeolian sand transport and sedimentation dynamics in the Danghe Reservoir area. Sedimentation rates varied markedly among sites: the sand-dune plot on Mingsha Mountain recorded a peak of 13.5 kg·month^{-1} in November, reflecting the highest local wind speeds. The right bank, dominated by fine particles (20.48% in the 0.002–0.005 mm range), displayed very low and stable deposition of 0.05–0.06 kg·month^{-1}, indicating weaker winds. By contrast, the left bank accumulated 0.18–0.29 kg·month^{-1} and exhibited a more uniform grain-size spectrum, signalling greater transport potential. SEM analysis showed smoother grains on the right bank but more weathered, angular particles on the left bank and at Mingsha Mountain. Vertically, finer particles were concentrated in the upper layers, especially at 0.64–0.80 m. These findings show how wind regime and terrain jointly shape aeolian transport and deposition, offering guidance for sand-control measures and water-resource management in arid regions.

1. INTRODUCTION

Jiuquan City, located in the northwest arid region of China, is a typical aeolian low--pressure area. Due to its unique topography and climatic conditions, it has formed a complex aeolian sand flow system, especially along the edge of the Kumtag Desert and the

[1]School of Energy and Power Engineering, Lanzhou University of Technology, Lanzhou 730000, China, corresponding author Yu Wang, email address: wangyu-mike@163.com

[2]Key Laboratory of Ecohydrology of Inland River Basin, Northwest Institute of Eco-Environment and Resources, Chinese Academy of Sciences, Lanzhou 730000, China.

[3]Gansu Provincial Key Laboratory of Biomass Energy and Solar Energy Synergistic Supply Systems, Lanzhou 730050, China.

[4]Gansu Provincial Water Environment Monitoring Centre, Lanzhou 730000, China.

[5]Water Conservancy Project Construction Cost and Fee Management Center, Gansu Provincial Water Conservancy Department, Lanzhou 730046, China.

banks of the Danghe Reservoir [1]. In these regions, aeolian sand particles are transported by boundary-layer processes, including turbulence, shear layer instability, and vortex motion under strong winds [2]. In this study, the term "aeolian sand" refers to wind-blown sand particles. Ultimately, these particles are deposited in river channels and reservoirs. The accumulated sediments in the river channels and reservoirs not only affect the river morphology and reservoir capacity but may also lead to increased water turbidity and ecosystem imbalance [3]. Therefore, in-depth research on the dynamic characteristics of aeolian sand and the movement patterns of aeolian sand entering the reservoir is crucial for developing effective aeolian sand control measures and water resource management strategies.

In the process of aeolian sand transport and deposition into the river and reservoir in the aeolian low-pressure area, sand particles of different sizes are transported in various ways, such as saltation, suspension, and traction flow, under the influence of wind speed, topography, and local flow field characteristics [4]. Ultimately, these particles deposit in the river and reservoir. The movement trajectories and dynamic behaviors of aeolian sand particles in the boundary layer are influenced by shear stress, turbulence intensity, and vorticity, especially under the effect of changes in wind speed and direction [5]. The variations in flow velocity gradients result in significant differences in the thickness and distribution characteristics of the sediment layers, displaying complex transport paths and deposition patterns. Additionally, the vertical particle size distribution and sediment layer differentiation reflect the dynamic characteristics of aeolian sand particles during their movement and deposition processes [6]. Larger particles, due to gravitational forces, settle more quickly to the ground, while smaller particles, supported by turbulence and airflow, can remain at higher altitudes and be transported over greater distances [7]. This vertical distribution characteristic causes sediment layers to show clear stratification at different heights and locations, forming complex particle size gradients in the river and reservoir sediment structures [8]. As wind speed, turbulence intensity, and topographical conditions change, the vertical particle size distribution also adjusts, further intensifying the spatial heterogeneity of the deposition pattern.

Existing studies have provided valuable insights into the transport patterns of aeolian sand in complex dynamic environments [9]. However, traditional research methodologies have proven to be less effective in controlling sediment transport into rivers and reservoirs under the extreme aeolian sand conditions characteristic of the northwest low-pressure region of China. Much of the previous research has primarily focused on the aeolian sand flow characteristics in desert margins or specific river areas. For instance, studies of the Kubuqi Desert and the Taklamakan Desert have showed key transport patterns and deposition features of aeolian sand [10]. These studies predominantly concentrate on the transport mechanisms at desert-oasis boundaries, limiting their scope to aeolian sand dynamics within desert environments. There is, however, a notable gap in research regarding sedimentary characteristics during the aeolian sand transport process when entering rivers and reservoirs. Furthermore, existing dust deposition studies have mainly examined the

spatial distribution of sediment thickness over large areas, with little attention paid to vertical distribution, settling characteristics, or the impact of fine particles on river and reservoir sediment structures. These aspects remain underexplored, particularly in terms of their effects on water bodies in arid and semi-arid regions. As such, detailed investigations into the aeolian sand dynamics and deposition mechanisms around the Danghe Reservoir are crucial.

The primary goal of this research was to (1) analyze the effects of wind speed, wind direction, and turbulence structure on aeolian sand transport and deposition; (2) investigate the vertical distribution characteristics of aeolian sand and its sedimentation mechanisms in river and reservoir environments; and (3) evaluate the coupling relationships between turbulence structures, topographical features, and grain size settling patterns during aeolian sand transport.

2. OVERVIEW OF THE STUDY AREA

Danghe Reservoir, located in Jiuquan City, Gansu Province, in the arid northwest of China (Fig. 1), is a typical area with high occurrences of wind erosion and sand damage. The Danghe Reservoir area experiences an arid climate with sparse rainfall, averaging less than 150 mm per year, while evaporation exceeds precipitation by a significant margin, reaching approximately 2,000 mm annually [11]. This extreme moisture deficit results in a scarcity of surface water resources, making the reservoir and surrounding areas highly vulnerable to wind erosion and sandstorms.

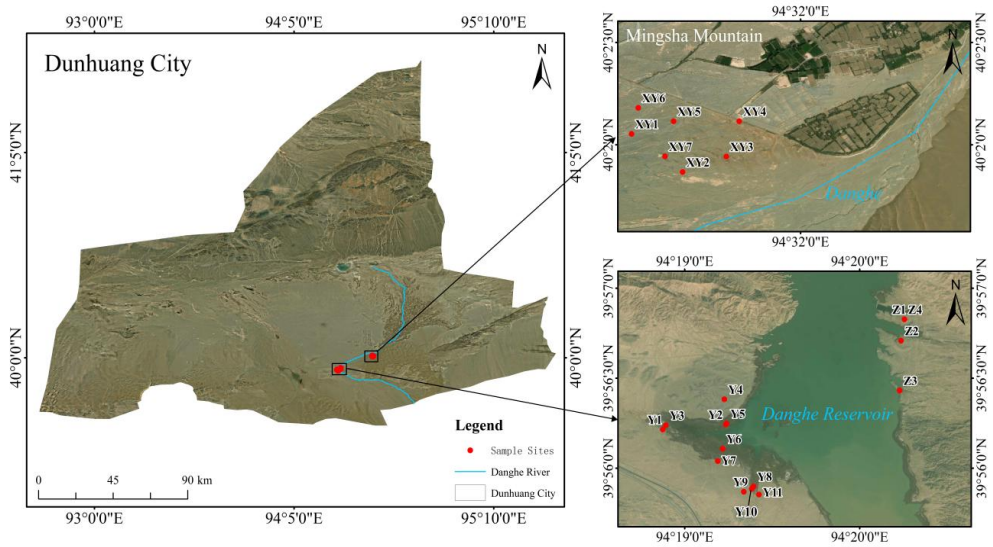

Fig. 1. Overview of the study area

Vegetation along the shores of the Danghe Reservoir is sparse, primarily consisting of drought-resistant herbaceous plants. Desertification and land degradation are evident in the area. The Mingsha Mountain, a typical dune area around the Danghe Reservoir, is characterized by its distinctive landforms, formed by the accumulation of fine sand. The dunes can reach heights of several tens of meters and serve as one of the primary sources of wind-blown sand for the reservoir area.

As illustrated by the study area map (Fig. 1) and the coordinates listed in Table 1, three primary zones were targeted around the Danghe Reservoir: the left bank, the right bank, and the Mingsha Mountain region. These zones were selected because they encompass the main corridors of aeolian sand transport and represent distinct geomorphic settings that directly influence sediment movement into the reservoir.

Table 1

Sampling points in the study area

Sampling point		Geographic coordinates	Sampling point		Geographic coordinates
Right bank of the reservoir	Z1	39.947120° N, 94.337598° E	Left bank of the reservoir	Y1	39.936918° N, 94.314580° E
	Z2	39.945137° N, 94.337267° E		Y2	39.937382° N, 94.320588° E
	Z3	39.940533° N, 94.337143° E		Y3	39.937313° N, 94.314882° E
	Z4	39.947120° N, 94.337598° E		Y4	39.939712° N, 94.320450° E
Mingsha Mountain	XY1	40.034995° N, 94.522842° E		Y5	39.937475° N, 94.320658° E
	XY2	40.031892° N, 94.527115° E		Y6	39.935130° N, 94.320295° E
	XY3	40.033152° N, 94.530783° E		Y7	39.933990° N, 94.319818° E
	XY4	40.036026° N, 94.531860° E		Y8	39.931650° N, 94.323227° E
	XY5	40.036026° N, 94.526367° E		Y9	39.931145° N, 94.322298° E
	XY6	40.044795° N, 94.519886° E		Y10	39.931418° N, 94.323047° E
	XY7	40.033165° N, 94.525642° E		Y11	39.930893° N, 94.323748° E

Sites Y4 (slope) and Y5 (gully) are adjacent sampling points at the slope–gully transition; despite similar GPS coordinates, they represent distinct micro-landforms.

Left bank (i.e., the southern shore of the reservoir) features relatively accessible terrain and notable variability in vegetation cover near the shoreline. The right bank (i.e., the northern shore of the reservoir) has narrower floodplain zones and experiences slightly different prevailing winds due to local topographic steering.

Mingsha Mountain Region, known to be a significant source of wind-blown sand in the broader landscape, serves as an upwind dune system contributing sediment toward the reservoir. Placing instruments in this dune environment enables assessment of the initial sediment supply and transport dynamics before sand reaches the reservoir periphery.

The monitoring points in the right bank area include Z1 (39.947120° N, 94.337598° E), where the bucket and sand sample collection devices were set up; Z2 (39.945137° N, 94.337267° E), which is a bucket sampling point; and Z3 (39.940533° N, 94.337143° E) and Z4 (39.947120° N, 94.337598° E), where both bucket and sand sample collection equipment was deployed.

In the left bank area, the following sampling points were set up: Y1 (39.936918° N, 94.314580° E), which is a meteorological station and sand collection device point; Y2 (39.937382° N, 94.320588° E), a bucket sampling point near the forest edge close to the road; Y3 (39.937313° N, 94.314882° E), a bucket sampling point located inside the forest; Y4 (39.939712° N, 94.320450° E), a sand collection device and bucket point on the slope; Y5 (39.937475° N, 94.320658° E), a large sand bucket point in the gully (bucket broken, no statistical data); Y6 (39.935130° N, 94.320295° E), a double bucket sampling point; Y7 (39.933990° N, 94.319818° E), a sand collection device and bucket point; Y8 (39.931650° N, 94.323227° E), located inside the forest belt with sand collection device and bucket; Y9 (39.931145° N, 94.322298° E), a bucket point outside the forest belt near the road; Y10 (39.931418° N, 94.323047° E) and Y11 (39.930893° N, 94.323748° E), located outside the forest belt. This setup ensured comprehensive data collection from a variety of locations within the left bank area.

The sampling points in the Mingsha Mountain area are densely arranged to monitor dune dynamics and sediment characteristics. XY1 (40.034995° N, 94.522842° E) is located by the roadside and serves as a bucket sampling point (bucket broken, no statistical data); XY2 (40.031892° N, 94.527115° E) includes a meteorological station, sand collection device, and bucket sampling point; XY3 (40.033152° N, 94.530783° E) is a bucket sampling point, with another point at XY3 (40.033875° N, 94.531562° E) located inside the forest belt; XY4 (40.036026° N, 94.531860° E) is the site for a grass square sand trap experiment; XY5 (40.036026° N, 94.526367° E) is the site for a wooden pole sand trap experiment; XY6 (40.044795° N, 94.519886° E) is the location for a stone sand trap (bucket broken, no statistical data); XY7 (40.033165° N, 94.525642° E) is located at the end of the bare sand area of the dune.

Danghe Reservoir and its surrounding areas are of significant ecological and water resource management importance, while also facing threats from wind and sand deposition that affect reservoir capacity and the ecosystem. This study systematically monitors and analyzes the particle size distribution and deposition characteristics of windblown sand through the deployment of multiple sampling points in the left bank, right bank, and Mingsha Mountain areas. The goal is to uncover the dynamic mechanisms and sedimentation patterns during the aeolian sand transport and deposition process into the reservoir. These data will provide crucial support for developing more scientifically-based aeolian sand control measures and water resource protection strategies.

3. DATA AND METHODS

3.1. WIND SPEED AND DIRECTION DATA

The wind speed and direction data were collected from two high-precision automatic meteorological stations deployed in the Danghe Reservoir area, located at the left bank of

the reservoir (39.936918° N, 94.314580° E) and the Mingsha Mountain area (40.031892° N, 94.527115° E) (Fig. 2). At both stations, wind speed and direction were measured at a height of 2.0 m above ground level, ensuring comparability between the two datasets. Data collection from both stations occurs hourly, providing high-resolution time-series data of wind speed and direction.

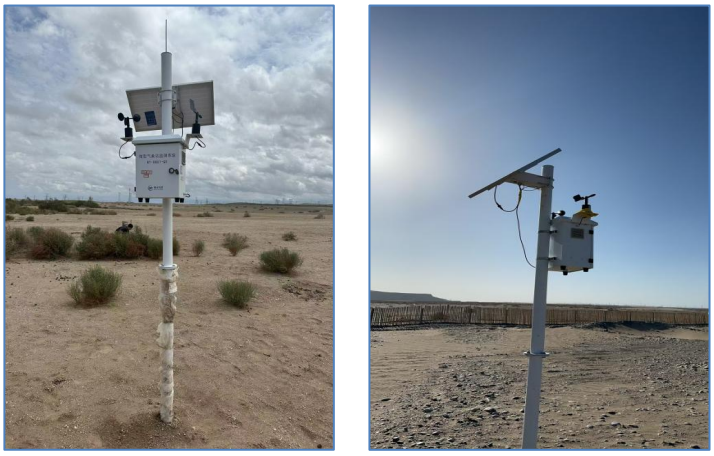

Fig. 2. On-site installation of meteorological stations

These stations represent the typical aeolian sand dynamics of riverbank and dune wind fields. The meteorological stations were provided by Jiangxi Nanyi Technology Co., Ltd. The accuracy of the wind speed (v) and direction sensors, with an error range of $\pm(0.3 + 0.03v)$ m/s for wind speed and ±2° for wind direction, was evaluated in the context of the study requirements. Although these accuracies are considered reasonable for capturing the general aeolian sand dynamics, potential errors within the range could have a minor impact on the detailed analysis of short-term and local aeolian sand interactions. Therefore, in the data analysis, we employed statistical methods to account for the possible errors and ensure the reliability of the results. Data collection from both stations occurs hourly, providing high-resolution time-series data of wind speed and direction. Wind speed and direction data show the dominant wind direction and wind shear stress distribution in the region, laying the data foundation for subsequent analysis of aeolian sand transport paths, boundary layer turbulence characteristics, and airflow dynamics.

3.2. SEDIMENT SAND DATA AND VERTICAL DISTRIBUTION SAND DATA

Sediment sand data. The sediment sand particle size data were obtained through sand collection bucket sampling. The sampling points were distributed across the left bank, right bank, and the Mingsha Mountain region of the Danghe Reservoir, covering different landform types and aeolian sand sedimentation environments within the reservoir area.

The sand collection buckets used in the study had a diameter of 0.2 m and were designed according to standardized specifications. To ensure the accuracy of the sand and dust collection, the buckets were buried to a depth of 0.015 m in the ground according to the standard requirements, preventing disturbances from the wind and sand (Fig. 3).

Fig. 3. Sand collection bucket layout and collection diagram

The sampling period for the sand collection buckets was set to daily and monthly cumulative totals to capture the variations in aeolian sand sedimentation over different time scales. After each sampling period, each bucket was cleaned and weighed, and the daily and monthly accumulated sand data were recorded. This data was used to analyze the influence of wind speed, wind direction, and terrain on sedimentation and particle size distribution.

Using a laser particle size analyzer, the particle size range was measured from 0.1 to 500 μm, covering fine sand particles to coarser gravel. The accumulated particle size distribution data and aeolian sand sedimentation amounts show transport and sedimentation patterns as well as spatial heterogeneity of wind and sand across different terrains and landform units.

Vertical distribution of sand data. The vertical distribution data were obtained using sand-collection instruments deployed at the Danghe Reservoir and adjacent dune–bank areas (Fig. 4). The samplers were the QN-JSY model (Shandong Qinong Information Technology Co., Ltd., China). Each unit had a total height of 1.30 m and an effective collection height of 0.80 m. Five vertical layers were defined within the effective height

to resolve the near-surface gradient of seolian (aeolian) transport: layer 1: 0–0.16 m, layer 2: 0.16–0.32 m, layer 3: 0.32–0.48 m, layer 4: 0.48–0.64 m, and layer 5: 0.64–0.80 m (center heights: 0.08, 0.24, 0.40, 0.56, and 0.72 m, respectively). The sampler collected sand through five rows of intake channels (10 channels per row; each channel 50 × 50 mm, vertical spacing 60 mm). The outer casing was 1.0-mm stainless steel to ensure mechanical stability under strong winds, and each collection bag had a capacity higher than 1,000 g, sufficient for daily and monthly deployments without overflow.

Fig. 4. Sand collection instrument layout and collection diagram (partial)

The sampling points were distributed across various landforms and sand activity zones, ensuring the representativeness and spatial diversity of the data. Each sand collection instrument was set to monitor on a daily and monthly cycle, recording the sand accumulation and particle size distribution at different height layers. Particle size distribution was determined using a Mastersizer 3000 (Malvern Instruments, UK), which measured particle sizes in the range of 0.01–2,000 μm with an accuracy of ±1%. Samples were introduced following the manufacturer's standard operating procedure, and each measurement was performed at least three times to ensure reproducibility.

3.3. SEDIMENT MICROSTRUCTURE DATA

The microstructural data of the sediments were analyzed using a scanning electron microscope (SEM), primarily to study the surface characteristics and morphological features of the sedimentary sand particles. The SEM used in this study is the Gemini SEM 500 model, produced by Zeiss, which offers high resolution and magnification, capable of clearly displaying the microstructure of the particles. The equipment had an adjustable accelerating voltage, typically set at 15 kV, to accommodate the observation needs of different types of sediment particles. The instrument's resolution was up to 1 nm, with a maximum magnification of 800,000 times, allowing detailed visualization of surface roughness, cracks, weathered layers, and other fine details of the particles. Surface morphology imaging is performed using the secondary electron detector (SE), while the backscattered electron detector (BSE) provides information on elemental distribution and surface composition.

SEM image analysis was used to examine weathering, abrasion, surface morphology changes, and sand transport and deposition patterns.

3.4. DATA ANALYSIS METHODS

This study employed various high-precision data analysis methods, combining wind speed, wind direction, sediment particle size distribution, vertical distribution, and SEM image analysis to investigate the aeolian sand flow characteristics, sedimentation patterns, and microstructure in depth.

Vertical distribution data collected by the sand collection devices were subjected to stratified statistical analysis to study the sedimentation patterns at different height levels. In the process of aeolian sand transport, larger particles generally tend to settle in lower layers closer to the surface, while smaller particles are more easily affected by turbulence and airflow, being suspended to higher levels and transported over longer distances. This is closely related to the shear force of airflow, turbulence intensity, and particle settling velocity [12].

Correlation analyses were conducted using monthly-averaged wind speed and corresponding monthly-averaged grain size data from each site. For each month (September, October, November), the daily data from stations within the same area were averaged to generate a single representative value. Thus, each area yielded three monthly data points for correlation analysis. This approach was repeated for each zone (left bank, right bank, dune). Monthly averages were chosen to account for short-term fluctuations and to focus on longer-term trends. To verify whether the observed differences in sediment grain size (or deposition rates) among the left bank, right bank, and dune area were statistically significant, a one-way ANOVA ($\alpha = 0.05$) was conducted on the monthly-averaged data. Post-hoc Tukey tests were employed to determine pairwise differences where applicable.

To analyze the sedimentation characteristics at different height levels, this study calculated the sediment accumulation at each level and, by combining wind speed and direction data at these levels, revealed the spatial heterogeneity of aeolian sand deposition in the vertical direction. Through these analyses, the study effectively uncovered the vertical distribution patterns of aeolian sand sedimentation and their variation trends at different heights, providing theoretical support for the optimization of aeolian sand control measures and protective structures.

4. RESULTS AND ANALYSES

4.1. WIND SPEED, WIND DIRECTION, AND THE CHARACTERISTICS OF AEOLIAN SAND TRANSPORT AND DEPOSITION

Based on the analysis of wind speed and direction data from typical days, the results indicate that the seasonal variations in wind speed and direction have a notable impact on aeolian sand transport in this area (Figs. 5 and 6).

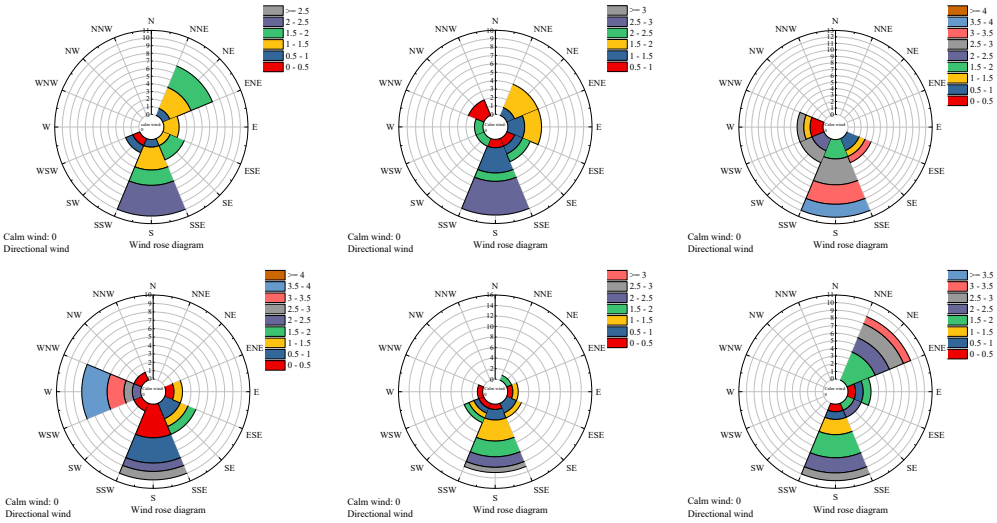

Fig. 5. Wind speed (in m/s) and wind direction rose diagrams on the left bank of the reservoir

Wind speeds on the left bank generally ranged from 1.0 to 2.5 m/s, with NW winds observed 35% of the time. Although other directions also occurred, NW remained the most frequent during September's typical days. We have included daily wind rose diagrams to illustrate these variations in wind direction and speed. In particular, during September and October, wind speeds were relatively low, with average speeds ranging from 1.0 to 2.5 m/s, and the predominant wind direction is northwest. During this period, the

aeolian sand transport capacity is weak, leading to the dominance of relatively coarse particles, a more localized deposit pattern, and a reduced transport distance. As November approaches, wind speeds increase to a range of 1.0–3.5 m/s, and the frequency of southeast winds (120–150°) notably increases. The enhanced wind speed strengthens the transport capacity of aeolian sand, allowing finer particles to be transported over longer distances. The increased wind speed not only boosts the transport capacity but also alters the sediment distribution patterns, resulting in finer particles being transported farther, with a broader range of particle size distribution.

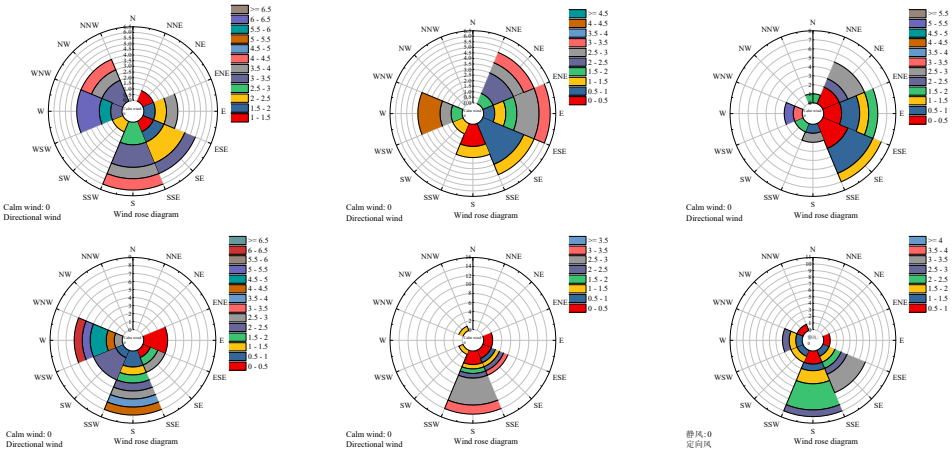

Fig. 6. Wind speed (in m/s) and wind direction rose diagrams for typical days on the sand dune

In the dune area, changes in wind speed have a particularly direct impact on aeolian sand transport. From September to October, although the wind speed is generally low, gusts can reach a maximum of 6.26 m/s. These short bursts of strong winds significantly promote the long-distance transport of fine particles. Additionally, changes in turbulence structure under higher wind speed conditions play a crucial role in aeolian sand transport. Enhanced turbulence intensity under high wind speeds significantly increases the transport distance of fine particles.

4.2. SEDIMENT GRAIN SIZE DISTRIBUTION CHARACTERISTICS AND DEPOSITION MECHANISMS

Grain size distribution characteristics at different regions and depths. The grain size distribution of sediments forms an essential foundation for analyzing aeolian sand transport, deposition patterns, and their impacts on the ecological environment. Due to the relatively close distribution of regional sampling points and the insignificant differences in particle sizes among them, this study selected the right bank, left bank, and dune area for typical analysis. The distribution of grain size ranges and related deposition patterns in each region are shown in Fig. 7.

Analysis of sediment grain size distribution in the Danghe Reservoir's right bank, left bank, and dune areas shows significant differences in particle size composition across regions. The findings indicate that the right bank's grain size distribution is concentrated in the finer particle range, with 0.002–0.005 mm particles accounting for 20.48% and 0.010–0.020 mm particles accounting for 12.35%. It seems that lower wind speeds on the right bank favor the deposition of fine particles, while the proportion of larger particles deposited is minimal (e.g., 0.200–0.300 mm particles account for only 0.34%).

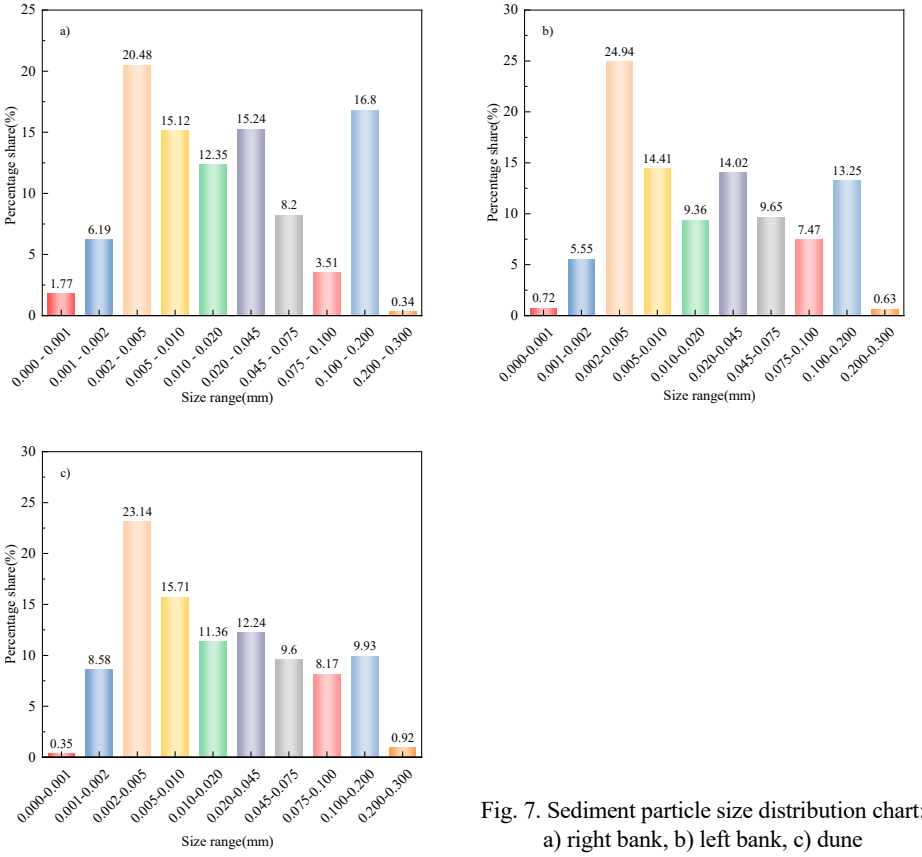

Fig. 7. Sediment particle size distribution chart: a) right bank, b) left bank, c) dune

On the left bank, the grain size distribution is relatively uniform. Fine particles (0.002–0.005 mm and 0.010–0.020 mm) have a high proportion, accounting for 24.94% and 9.36%, respectively, while medium-sized particles (0.020–0.045 mm) also occupy a substantial proportion (14.02%). This indicates moderate wind speeds in this area, which effectively transport and deposit particles of varying sizes.

In the dune area, the grain size distribution is more diverse. Fine particles still account for a significant proportion, at 23.14% and 15.71%, respectively. However, compared to the right and left banks, the proportion of 0.001–0.002 mm particles in the dune area

increases significantly (to 8.58%). Additionally, medium and larger particles, such as 0.020–0.045 mm (12.24%) and 0.100–0.200 mm (9.93%), are deposited at higher proportions. By setting up multiple monitoring points of the Danghe Reservoir, aeolian sand data at different height layers were collected (Fig. 8).

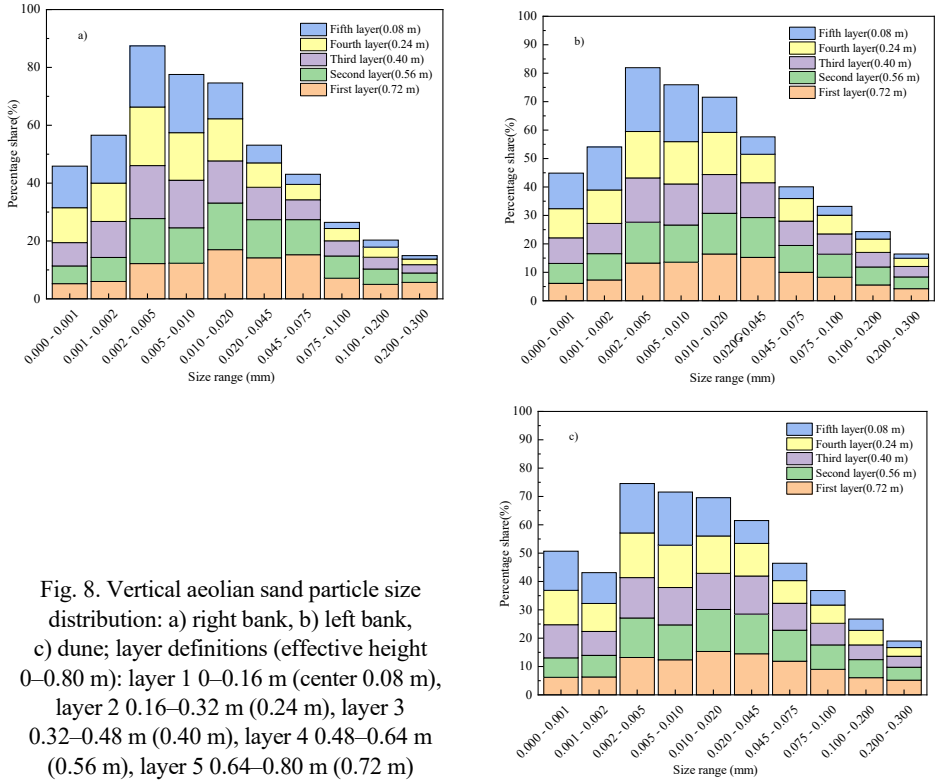

Fig. 8. Vertical aeolian sand particle size distribution: a) right bank, b) left bank, c) dune; layer definitions (effective height 0–0.80 m): layer 1 0–0.16 m (center 0.08 m), layer 2 0.16–0.32 m (0.24 m), layer 3 0.32–0.48 m (0.40 m), layer 4 0.48–0.64 m (0.56 m), layer 5 0.64–0.80 m (0.72 m)

Aeolian sand deposition in these regions showed variations in grain size distribution with height. Coarse particles tend to deposit in the lower layers, while finer particles primarily settle at higher layers. Monitoring data show that larger particles (e.g., 0.200–0.300 mm) are predominantly concentrated in the lower layers of 0–0.16 m and 0.16–0.32 m. Smaller particles (e.g., 0.000–0.005 mm) exhibit a significantly higher proportion of deposition in the upper layers (e.g., 0.64–0.8 m).

Sedimentation mechanisms of dunes in different regions. A systematic analysis of sediment data from monitoring points around the Danghe Reservoir was conducted to explore the variations in aeolian sand deposition. Daily sedimentation data from September 1 to December 1 were recorded, and the monthly sand accumulation for September, October, and November was calculated based on these daily records (Fig. 9). The daily sand deposition data show significant spatial differences in sand accumulation across regions. The

dune area exhibited a noticeably higher deposition rate than the left bank, particularly from September to November, with significant seasonal variations. In the dune area, the deposition rate remained relatively stable at 12.7 kg in September and 13.0 kg in October but increased to 13.5 kg in November as wind speeds increased.

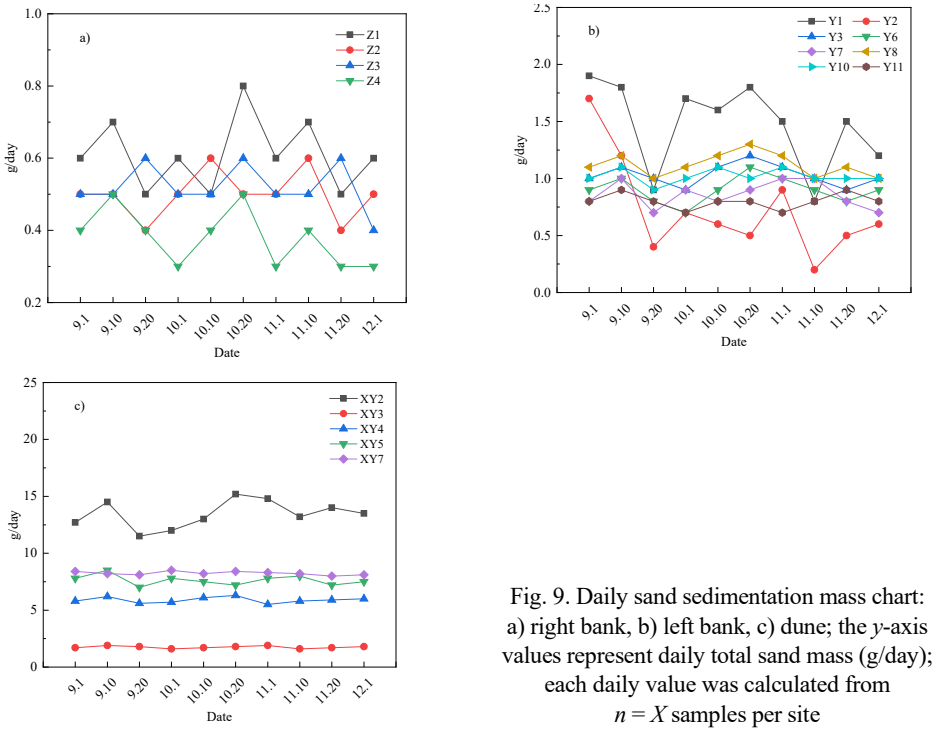

Fig. 9. Daily sand sedimentation mass chart: a) right bank, b) left bank, c) dune; the *y*-axis values represent daily total sand mass (g/day); each daily value was calculated from $n = X$ samples per site

Overall, seasonal variations in wind speed directly influenced the fluctuations in deposition rates. When wind speeds were higher, especially in the dune area, deposition rates increased significantly, highlighting the critical role of wind speed and topography in aeolian sand transport and deposition processes (Fig. 10).

Based on monthly aeolian sand accumulation data, significant spatial and seasonal variations in sand accumulation were observed across different locations within the study area. The dune area's monthly deposition showed a notable increase from September to November, peaking at 13.5 kg in November, reflecting the region's increased wind speed and sand transport capacity. In contrast, the right bank showed only 0.05–0.06 kg·month^{-1} of sand deposition throughout the period, with almost no month-to-month variation – evidence of steadier winds and a limited sand supply. The left bank, by comparison, increased modestly from 0.18 kg in September to 0.29 kg in November, indicating that the seasonal increase in wind strength slightly enhanced sediment capture and promoted gradual accumulation.

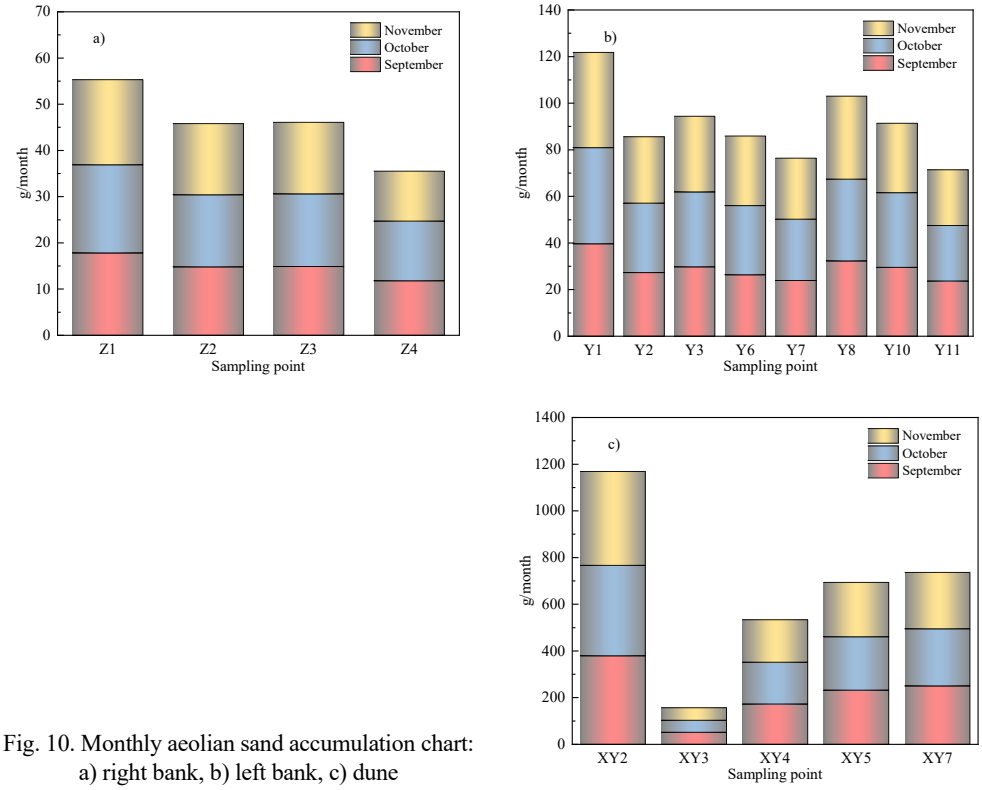

Fig. 10. Monthly aeolian sand accumulation chart: a) right bank, b) left bank, c) dune

4.3. SCANNING ELECTRON MICROSCOPE (SEM) ANALYSIS AND PARTICLE SURFACE CHARACTERISTICS

Using SEM, the surface characteristics of aeolian sand particles collected from different regions of the Danghe Reservoir were analyzed (Figs. 11–13).

Differences in surface features of particles from these regions were observed. Particles from the right bank exhibited relatively smooth surfaces with weaker weathering effects and minimal cracks or fissures. In contrast, particles from the left bank showed more pronounced weathering and fragmentation, with higher surface roughness and significant cracks and micropores, characteristics associated with higher wind speeds and longer transport distances. Particles from the dune area displayed more complex surface structures and more prominent weathering features, closely related to the higher wind speeds and intense aeolian sand transport processes in this region. These findings indicate that wind speed plays a crucial role in the weathering and fragmentation of particles, thereby influencing their deposition patterns.

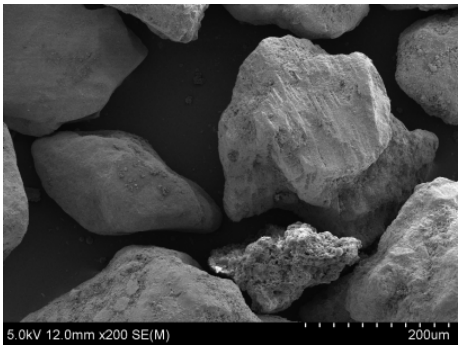

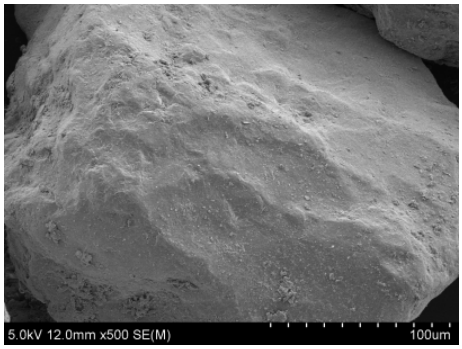

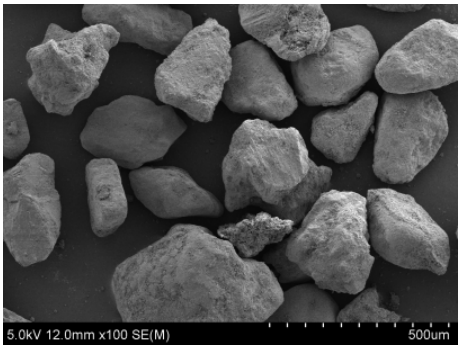

Fig. 11. SEM image of sedimentary aeolian sand particles from the right bank

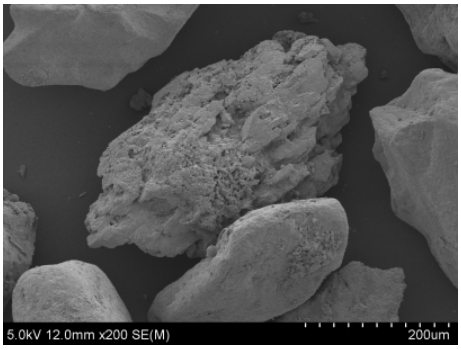

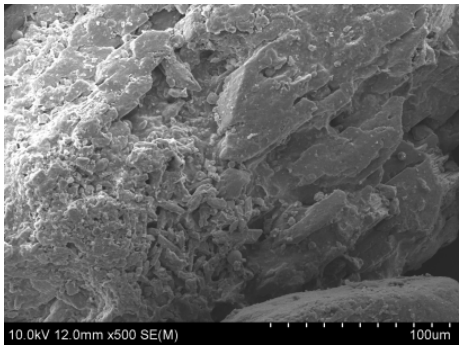

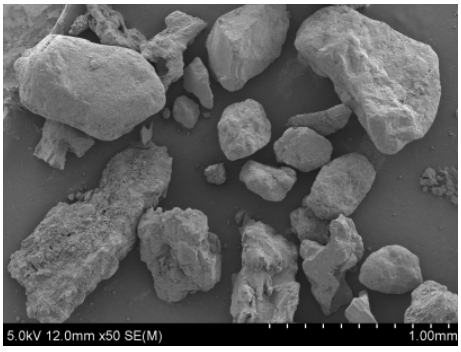

Fig. 12. SEM image of sedimentary aeolian sand particles from the left bank

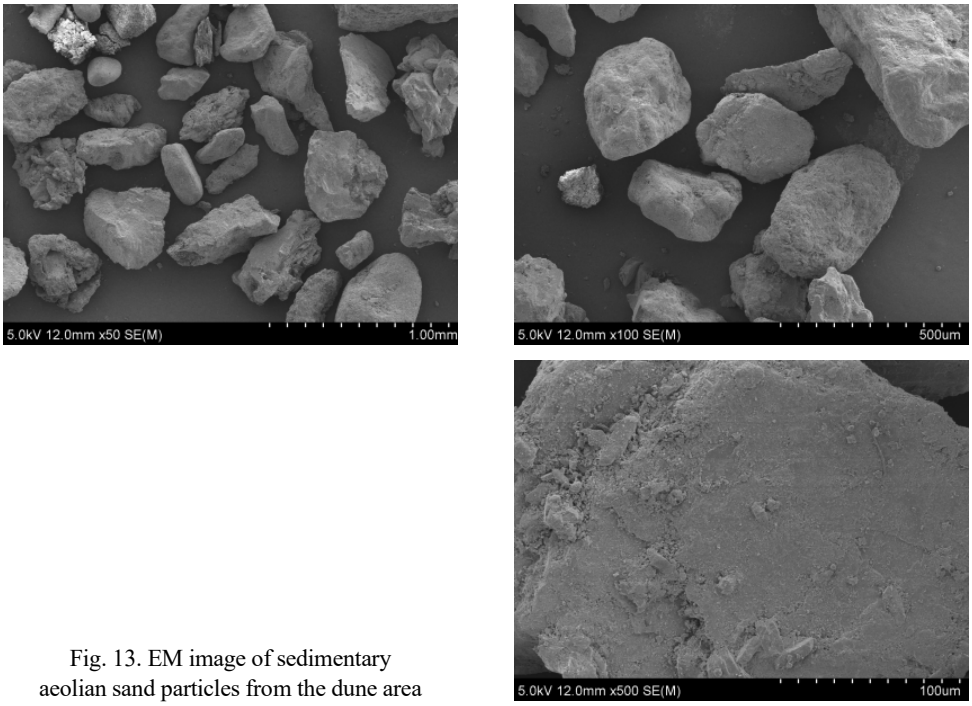

Fig. 13. EM image of sedimentary aeolian sand particles from the dune area

5. DISCUSSION

5.1. CORRELATION BETWEEN SEASONAL WIND SPEED AND SEDIMENT GRAIN SIZE DISTRIBUTION

Wind speed is one of the key factors influencing aeolian transport and sediment distribution, particularly in arid and semi-arid regions. The seasonal variations in wind speed significantly affect the distribution of sediment grain sizes. Through analyzing the correlation between wind speed and sediment grain size distribution, we found a clear seasonal variation, with wind speed having a more significant impact on finer particles than on coarser particles (Fig. 14). This result aligns with findings from other similar regions and provides valuable insight into understanding the aeolian sediment deposition characteristics in the study area.

Hourly wind records were aggregated and converted to monthly means for September, October, and November to minimise short-term variability. Grain-size data originated from monthly composite samples taken at three representative points – the right bank (Z3/Z4), the left bank (Y6), and the dune zone (XY5) – within the same September-to-November window. Pearson correlation coefficients (Fig. 14) were then derived by matching

each location's monthly-averaged wind speed with the corresponding monthly fractions of fine, medium, and coarse particles.

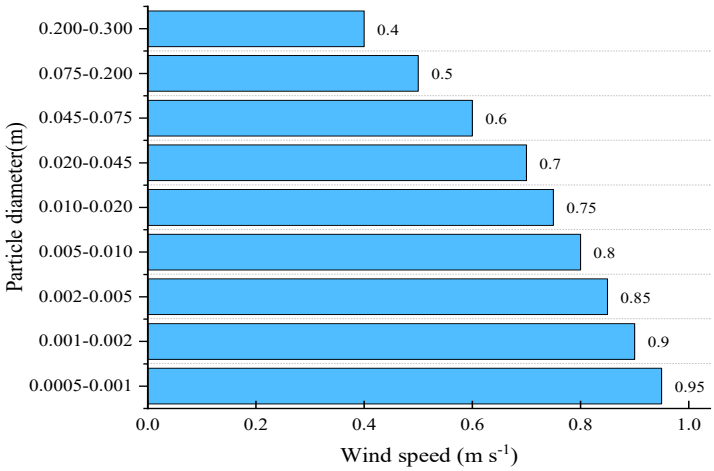

Fig. 14. Correlation between wind speed and grain size range

From the data presented in the chart, the Pearson correlation coefficients between wind speed and smaller sediment particles (such as 0.0005–0.001 mm, 0.001–0.002 mm) are high, with values of 0.95 and 0.90, respectively. This indicates that, during periods of lower wind speeds, fine particles are more directly affected by wind speed changes. This observation aligns with Wang et al. [15], who found that during stronger wind conditions, fine particles (such as dust) in the desert fringe areas are more likely to accumulate, and finer particles are transported over longer distances. In our study area around Danghe Reservoir, similar seasonal wind speed changes caused fine particles to show notable seasonal differences in deposition.

5.2. AEOLIAN SAND DEPOSITION CHARACTERISTICS IN THE RIGHT BANK, LEFT BANK, AND DUNE AREA

The study of aeolian sand deposition characteristics across the Danghe Reservoir shows distinct patterns driven by varying wind speeds, sediment grain sizes, and topographical conditions (Fig. 15).

On the right bank, the grain size distribution is dominated by fine particles, particularly in the 0.002–0.005 mm and 0.010–0.020 mm size ranges, which account for 20.48% and 12.35%, respectively. This trend is attributed to the relatively low wind speeds in this area, which are insufficient to transport larger particles efficiently. In fact, the larger particle sizes, such as 0.200–0.300 mm, make up only 0.34% of the total deposition. The correlation matrix further reinforces this by showing strong negative correlations between finer particles (0.000–0.001 mm) and coarser ones (0.075–0.100 mm, –0.99). The fine

particles are more prone to deposition under low wind conditions, while coarse particles are less likely to settle in these regions.

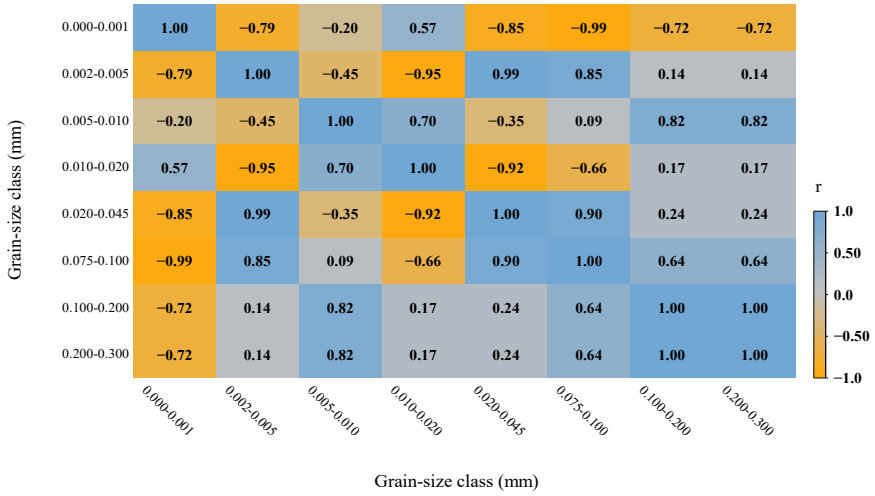

Fig. 15. Correlation matrix of aeolian sand particle size distribution

This result aligns with other studies [16]which suggest that lower wind speeds typically result in the deposition of finer sand fractions, as the wind's transport capacity is insufficient to carry larger grains over long distances. These studies emphasize the significance of wind velocity in controlling the grain size distribution in arid and semi-arid environments, where wind erosion is a critical factor. In contrast to the right bank, the moderate wind speeds in the left bank promote a greater diversity in particle sizes, as observed by other researchers [17]. Their study in similarly arid regions noted that moderate wind conditions lead to the transport and deposition of both fine and medium-sized particles, with the deposition pattern being more heterogeneous. This aligns with our findings, where moderate winds facilitate the distribution of a broader spectrum of sediment sizes.

These findings are consistent with previous studies on desert environments, such as those by Li et al. [19], who demonstrated that dunes act as a source of both fine and coarse particles. In areas with higher wind speeds, larger particles are often transported over shorter distances, while finer particles are carried farther by the wind. This dual process of fine and coarse sedimentation in dunes has been well-documented in other arid regions and is critical to understanding the dynamics of sediment transport in desert environments.

In conclusion, the sediment deposition characteristics observed in this study align with existing research on aeolian sand transport in arid environments, with wind speed and topography playing crucial roles in determining sediment grain size distribution. Understanding these patterns is essential for the development of effective erosion control and dune management strategies in desert regions like the Danghe Reservoir.

6. CONCLUSIONS

Higher wind speeds in November (1.0–3.5 m/s) facilitated the long-distance transport of finer particles (0.002–0.005 mm), while lower wind speeds in September and October favored localized deposition of coarser fractions. These results underscore the pivotal role of wind speed in shaping grain size distributions, particularly in arid environments prone to significant seasonal fluctuations.

The dune area exhibited substantially higher sediment accumulation and a broader particle size spectrum, reflecting its stronger winds and direct contribution of sand to the reservoir. In contrast, the right bank, with more moderate winds, saw lower overall deposition and a predominance of finer fractions. The left bank displayed relatively uniform grain size distributions, suggesting an intermediate transport capacity.

Vertical sampling showed stratification with coarse grains (e.g., 0.200–0.300 mm) concentrated at lower heights, whereas finer particles were abundant in the upper layers. SEM observations further indicated that elevated wind intensities promote mechanical weathering and roughened particle surfaces, linking wind regimes to the microstructural evolution of aeolian sand.

By delineating how wind speed and topography control both the spatial and vertical patterns of aeolian sand, this study highlights the need for targeted mitigation measures. Vegetation buffers or engineered barriers positioned in high-transport corridors (e.g., near dune areas) could curb reservoir infilling and safeguard water quality. However, field trials or numerical modelling will be necessary to quantify the actual effectiveness of such barriers in the specific topographic context of the Danghe Reservoir area. Future research should explore extended temporal coverage (beyond three months) and employ additional statistical metrics to refine our understanding of seasonal wind–sediment interactions in similar arid landscapes.

ACKNOWLEDGMENT

National Natural Science Foundation of China, Regional Fund: Study on the Mechanism of Heavy Metal Migration and Transformation in Alpine Inland Rivers Due to Cascading Dam Construction (Grant No. 52169015); China's National Key Research and Development Program: Targeted Depolymerization and Enhanced Pretreatment Technology for Diversified Biomass Alcohol Feedstocks (Grant No. 2022YFB4201901-1); Gansu Key Research and Development Program of China (Grant No. 23YFFA0020). This work was supported by Incubation Program of Excellent Doctoral Dissertation-Lanzhou University of Technology.

REFERENCES

[1] XIE S., QU J., PANG Y., *Causes and controlling pattern of sand hazards at the Danghe Reservoir of Dunhuang in Northwest China*, J. Mt. Sci., 2016, 13, 1973–1983. DOI: 10.1007/s11629-016-4067-3.

[2] KOK J.F., PARTELI E.J.R., MICHAELS T.I., BOU KARAM D., *The physics of wind-blown sand and dust*, Rep. Prog. Phys., 2012, 75 (10), 106901. DOI: 10.1088/0034-4885/75/10/106901.

[3] JURACEK K.E., *The aging of America's reservoirs: in-reservoir and downstream physical changes and habitat implications*, J. Am. Water Res. Assoc., 2015, 51 (1), 168–184. DOI: 10.1111/jawr.12238.
[4] BRAAT L., BRÜCKNER M.Z.M., SEFTON-NASH E., LAMB M.P., *Gravity-driven differences in fluvial sediment transport on Mars and Earth*, J. Geophys. Res. Planets, 2024, 129 (2), e2023JE007788. DOI: 10.1029/2023JE007788.
[5] HE W., ZHANG J., XU X., *Estimation of aerodynamic entrainment in developing wind-blown sand flow*, Sci. Prog., 2024, 107 (4), 368504241290970. DOI: 10.1177/00368504241290970.
[6] FARRELL E.J., SHERMAN D.J., ELLIS J.T., LI B., *Vertical distribution of grain size for wind-blown sand*, Aeolian Res., 2012, 7, 51–61. DOI: 10.1016/j.aeolia.2012.03.003.
[7] YU H., CHENG W., WU L., WANG H., XIE Y., *Mechanisms of dust diffuse pollution under forced-exhaust ventilation in fully mechanised excavation faces by CFD-DEM*, Powder Technol., 2017, 317, 31–47. DOI: 10.1016/j.powtec.2017.04.045.
[8] IJZENDOORN C.O., HALLIN C., COHN N., RENIERS A.J.H.M., DE VRIES S., *Novel sediment sampling method provides new insights into vertical grain-size variability due to marine and aeolian beach processes*, Earth Surf. Proc. Landf., 2023, 48 (4), 782–800. DOI: 10.1002/esp.5518.
[9] ABDALLA M.A.M., NOVELLINO A., HUSSAIN E., MARSH S., PSIMOULIS P., SMITH M., *The use of SAR offset tracking for detecting sand dune movement in Sudan*, Remote Sens., 2020, 12 (20), 3410. DOI: 10.3390/rs12203410.
[10] RITTNER M., VERMEESCH P., CARTER A., BIRD A., STEVENS T., GARZANTI E., ANDÒ S., VEZZOLI G., DUTT R., XU Z., LU H., *The provenance of Taklamakan desert sand*, Earth Planet. Sci. Lett., 2016, 437, 127–137. DOI: 10.1016/j.epsl.2016.02.045.
[11] LIN J., MA R., HU Y., SUN Z., PENG J., *Groundwater sustainability and groundwater/surface-water interaction in arid Dunhuang Basin, Northwest China*, Hydrogeol. J., 2018, 26 (11), 3309–3323. DOI: 10.1007/s10040-018-1743-0.
[12] LÜ H., SHAO Y., YANG X., *Impact of turbulence on aeolian particle entrainment: Results from wind-tunnel experiments*, Atmos. Chem. Phys., 2022, 22, 9525–9544. DOI: 10.5194/acp-22-9525-2022.
[13] KOK J.F., PARTELI E.J.R., MICHAELS T.I., BOU KARAM D., *The physics of wind-blown sand and dust*, Rep. Prog. Phys., 2012, 75 (10), 106901. DOI: 10.1088/0034-4885/75/10/106901.
[14] ZHANG J., LI G., SHI L., HUANG N., SHAO Y., *Impact of turbulence on aeolian particle entrainment: Results from wind-tunnel experiment*s, Atmos. Chem. Phys., 2022, 22, 9525–9535. DOI: 10.5194/acp-22-9525-2022.
[15] GILLETTE D.A., WALKER T.R., *Characteristics of airborne particles produced by wind erosion of sandy soil, high plains of West Texas*, Soil Sci., 1977, 123 (2), 97–110. DOI: 10.1097/00010694-197702000-00004.
[16] LI B., FENG Q., LI Z., WANG F., LUO C., LI R., HU H., *Provenance of surface dune sands in the Gurbantunggut Desert, northwestern China: Qualitative and quantitative assessment using geochemical fingerprinting*, Geomorphology, 2024, 452, 109115. DOI: 10.1016/j.geomorph.2024.109115.
[17] HUANG Y., KOK J.F., MARTIN R.L., SWET N., KATRA I., GILL T.E., REYNOLDS R.L., FREIRE L.S., *Fine dust emissions from active sands at coastal Oceano Dunes, California*, Atm. Chem. Phys., 2019, 19, 2947–2964. DOI: 10.5194/acp-19-2947-2019.